American Mineralogist, Volume 85, pages 1315–1320, 2000

Tegengrenite, a new, rhombohedral spinel-related Sb mineral from the Jakobsberg Fe-Mn deposit, Värmland, Sweden

DAN HOLTSTAM[1,*] AND ANN-KRISTIN LARSSON[2]

[1]Department of Mineralogy, Research Division, Swedish Museum of Natural History, Box 50007, SE-104 05 Stockholm, Sweden
[2]Department of Inorganic Chemistry, Arrhenius Laboratory, Stockholm University, SE-106 91 Stockholm, Sweden

ABSTRACT

Tegengrenite, forming octahedra up to 150 μm in size, occurs associated with hausmannite, calcite, brucite, dolomite, clinohumite, kinoshitalite, native copper, barytocalcite, bindheimite, and cerussite in Mn ore from Jakobsberg, Filipstad district, Värmland, Sweden. The mineral is deep red and translucent, with a sub-adamantine luster. In reflected light it is gray and nearly isotropic, with measured reflectance values (R%) 10.4 (λ = 470 nm), 10.0 (546 nm), 9.9 (589 nm), and 9.8 (650 nm). The refractive index at λ = 589 nm is 1.92(2). There is no cleavage; fracture is conchoidal. D_{calc} is 4.58(1) g/cm^3. Electron-microprobe analyses gave (average of 35 points; in wt%) MgO 21.83, Al_2O_3 0.76, SiO_2 1.70, Sb_2O_5 36.13, TiO_2 1.40, Fe_2O_3 0.78, MnO 25.74, Mn_2O_3 (calculated from stoichiometry) 8.14, ZnO 2.66, sum 99.14, yielding the empirical formula $Mg^{2+}_{1.22}Mn^{2+}_{0.82}Zn_{0.07}(Sb_{0.50}Mn^{3+}_{0.23}Si_{0.06}Ti_{0.04}Al_{0.03}Fe_{0.02})O_4$. Combined X-ray and electron diffraction studies show that tegengrenite is rhombohedral, space group $R\bar{3}$ or $R3$, and pseudocubic. The individual tegengrenite octahedra consist of eight twin domains that give rise to complex diffraction patterns and make them unsuitable for a conventional structure determination. Tegengrenite, like the chemically related mineral filipstadite, bears a close structural relationship to spinel. The eight strongest lines in the X-ray diffraction pattern are [d (in angstroms) (I/I_0)(hkl)]: 4.98(20)(211, 003), 4.32(19)(122), 4.24(18)(113), 3.052(33)(140, 214), 2.608(100)(241, 143, 125), 2.162(28)(244), 1.665(30)(363, 075), 1.531(26)(820) and 1.527(29)(428). The refined unit-cell parameters (hexagonal setting) are a = 16.196(1) and c = 14.948(2) Å with Z = 42; for the cubic spinel-type subcell $A = c/\sqrt{3}$ = 8.63 Å. The new species is named for Felix Tegengren (1884–1980).

INTRODUCTION

Filipstadite, with the ideal composition $Mn_2(Sb^{5+}_{0.5}Fe^{3+}_{0.5})O_4$, was described by Dunn et al. (1988) as a new spinel-related mineral from the Långban mine in the Filipstad district, Värmland, Sweden. A second occurrence of this rare species was reported from the Jakobsberg deposit of the same district by Holtstam (1993). In close association with the Jakobsberg filipstadite another phase (denoted "X" by Holtstam 1993) was observed, which apparently possessed chemical and structural similarities to filipstadite, but also had some distinct properties. A more detailed investigation of the second phase, which mostly appeared as a replacement product of filipstadite, was at that time hindered by the small sample volumes and its crystallographic coherency with the filipstadite host. A recent find of isolated, larger grains at Jakobsberg of this mineral makes a more complete characterization possible.

The new mineral is named tegengrenite in honor of Felix Tegengren (1884–1980), a renowned Finlandic-Swedish economic geologist. Among numerous missions, he was employed by the Geological Surveys of China and Sweden. His major written contributions were large synopses on ore deposits of those two countries (Tegengren 1921, 1924). The mineral and its name have been approved by the IMA Commission on New Minerals and Mineral Names. Holotype material is preserved at the Swedish Museum of Natural History, Stockholm, under the catalogue no. 980408.

OCCURRENCE AND PARAGENESIS

The material used for the present description is a mine dump sample found by the mineral collector Torbjörn Lorin of Örebro, Sweden. The Jakobsberg Fe-Mn oxide deposit (59.83°N, 14.11°E) is small-sized, and was mined sporadically mainly during the years 1891–1918, when 380 tons of Mn ore were taken out (Tegengren 1924). Hematite and hausmannite ore constitute separate, irregular bodies in association with different types of skarn and vein assemblages, partly consisting of minerals with Ba, Pb, As, Sb, B, or Be, or combinations of these elements, as essential components. Some more details on the mineralogy are given by Holtstam and Norrestam (1993). The host rock is an interbed of dolomitic marble, which belongs to a supracrustal, dominantly volcaniclastic rock formation of Palaeoproterozoic age (Svecofennian orogeny). Jakobsberg is counted as one of the Långban-type deposits (Moore 1970; Holtstam and Langhof 1999).

In the sample designated as the holotype specimen, hausmannite occurs as euhedral to subhedral crystals up to 1 mm across, irregularly dispersed in calcite marble, and partly in high concentration. The calcite is an Mn-bearing variety, showing a red-orange fluorescence color under short-wave UV light.

*E-mail: dan.holtstam@nrm.se

Flaky, colorless brucite is common, and tends to be coarsened (crystals up to 2 mm) in portions rich in carbonate. Brucite [with ca. 4 mol% of $Mn(OH)_2$] also appears as lamellar inclusions in hausmannite. Clinohumite, dolomite, native copper and kinoshitalite occur as scattered grains less than 1 mm in size. Minute grains of bindheimite and barytocalcite were detected in sections under the scanning-electron microscope, and identified utilizing an energy-dispersion microanalysis facility. Similarly, cerussite has been observed as thin alteration rims on dolomite grains.

Tegengrenite has a low modal abundance, but appears to be relatively evenly distributed in the samples studied. It sometimes occurs in aggregates of two or more grains, which are often in direct contact with hausmannite, but occasionally completely surrounded by carbonate (Fig. 1).

Physical and optical properties

Tegengrenite forms subhedral to euhedral grains, essentially octahedral in outline, and ranging from 30 to 150 μm in their greatest dimension. Neither cleavage nor parting was observed; fracture appears to be conchoidal. A density determination could not be carried out due to small grain size; a calculated value based on unit-cell contents is 4.58(1) g/cm^3.

Tegengrenite is a translucent mineral, with a deep red (ruby) megascopic color, and subadamantine luster. Under the microscope, in reflected linearly polarized light, it exhibits an undistinguished gray color, and has a significantly lower reflectivity than the coexisting hausmannite. Orange-red internal reflections are sometimes seen. Under crossed polars the mineral shows anisotropy, but the anisotropic nature is best seen in a thin section of standard thickness (transmitted light). It was not possible to determine the transmitted-light optical parameters, however, due to the presence of sector twinning. The approximately quadratic cross-sections usually consist of four sectors, each forming a triangle, and no positions with true extinction could be found.

Reflected-light properties were measured from a polished section. A Zeiss MPM800 microscope-photometer, fitted with a white light source and a photo-multiplier detector was used for data collection. An aperture was selected to give a field of measurement with a diameter of 20 μm. Ten consecutive spectral scans (10 nm steps) with a spectral resolution of 10 nm were made from 400 to 700 nm and automatically averaged. The data were corrected for parasitic-light effects and standardized against SiC (Zeiss no. 846). The variations in reflectance for different directions and on different grains are within ±0.3% absolute, which is comparable to the expected precision of the individual measurements. In reflected light, tegengrenite is thus practically isotropic, and only average values need to be reported. *R*% for the four wavelengths recommended by the IMA Commission on Ore Minerals are 10.4 (470 nm), 10.0 (546 nm), 9.9 (589 nm), and 9.8 (650 nm). For a non-opaque phase it is justified to assume that *k* (the absorption coefficient) is close to zero in the visible spectrum. Accordingly, the refractive index of tegengrenite has been calculated to 1.92(2) at 589 nm using the Fresnel equation (e.g., Cervelle and Moëlo 1990). The compatibility index calculated from the Gladstone-Dale relationship is –0.049, which falls in the "good" category (Mandarino 1981).

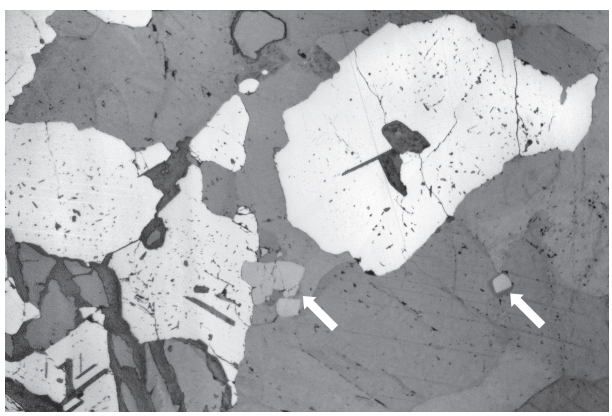

Figure 1. Photomicrograph of sample no. 980408 (reflected light). The light gray phase is hausmannite and the white arrows point to tegengrenite. The field of view is 1.5 × 1 mm.

Typical reflectance curves for tegengrenite (two directions in grain 1.1 analyzed chemically according to Table 1) are shown in Figure 2, which also includes data for filipstadite (Dunn et al. 1988). Both minerals are very weakly bireflectant, if at all, but for filipstadite there is a significant spread in the overall reflectance depending on the chemistry of the crystal measured; the two filipstadite curves represent samples that essentially differ in their Fe contents. For the present tegengrenite population the chemical variations are obviously not large enough to cause detectable fluctuations. Nevertheless, the reflectance of tegengrenite-filipstadite is to a large extent controlled by Fe^{3+}.

Chemical composition

The chemical composition of the new mineral was determined using wavelength dispersion analyses on a Cameca SX50 electron microprobe (Institute of Earth Sciences, Uppsala University) run with an acceleration voltage of 20 kV, a beam current of 12 nA, and a 1 μm beam diameter. Standards used were stibnite (Sb*L*α), $MnTiO_3$ (Mn,Ti*K*α), Fe_2O_3 (Fe*K*α), ZnS (Zn*K*α), MgO (Mg*K*α), Al_2O_3 (Al*K*α), and albite (Si*K*α). Data reduction was made using a Cameca version of the PAP (Pouchou and Pichoir 1984) routine. The accuracy of the measurements is expected to be better than ±2% relative of the major oxide components, and the precision is in the range 0.8–3%. Cr, V, and Ca were below the limit of detection (< 0.05 wt%). A total of 35 analyses were performed on six crystals of tegengrenite. The results are summarized in Table 1. Atomic proportions have been calculated assuming four O atoms per three cations. MnO and Mn_2O_3 could not be determined directly due to the small amount of sample, but was estimated from the stoichiometry. Fe is assumed to be in the trivalent state due to the generally oxidized state of the ores. For the same reason, we do not expect anion vacancies to be present in tegengrenite. The composition of a hausmannite grain in contact with tegengrenite was determined to be $Mn^{2+}_{0.86}Zn_{0.08}Mg_{0.06}(Mn^{3+}_{1.97}Fe_{0.02}Al_{0.01})_{\Sigma 2.00}O_4$. The Mg/(Mg + Mn) ratio for coexisting clinohumite is 0.94.

There is no major compositional heterogeneity among the

TABLE 1. Chemical analyses (wt%) of tegengrenite

Grain	1.1 $n = 10$	Range	1.2 $n = 6$	2.1 $n = 3$	2.2 $n = 8$	2.3 $n = 6$	2.4 $n = 2$	Grand mean $n = 35$	σ
MgO	22.04	21.69–22.32	21.74	21.51	21.81	21.70	21.88	21.83	0.38
Al_2O_3	0.73	0.60–0.83	0.74	0.76	0.79	0.80	0.69	0.76	0.07
SiO_2	1.65	1.57–1.80	1.65	1.72	1.89	1.57	1.73	1.70	0.13
Sb_2O_5	36.23	35.82–36.87	36.02	35.85	36.21	36.08	36.30	36.13	0.50
TiO_2	1.44	1.28–1.61	1.55	1.32	1.16	1.55	1.43	1.40	0.19
Fe_2O_3	0.82	0.65–0.92	0.83	0.89	0.62	0.85	0.64	0.78	0.14
MnO	25.46	24.62–25.85	26.02	25.86	25.94	25.80	25.58	25.76	0.54
Mn_2O_3	7.98	7.22–8.63	8.21	8.11	8.37	8.08	7.66	8.12	0.73
ZnO	2.59	2.33–2.80	2.59	2.60	2.71	2.78	2.81	2.66	0.15
Sum	98.93	98.52–99.43	99.35	98.61	99.50	99.22	98.72	99.14	0.51
Atomic proportions									
Mg	1.231		1.211	1.208	1.212	1.211	1.226	1.218	0.019
Al	0.032		0.032	0.034	0.035	0.036	0.031	0.033	0.003
Si	0.062		0.062	0.065	0.071	0.059	0.065	0.064	0.005
Sb	0.504		0.500	0.502	0.502	0.502	0.507	0.502	0.007
Ti	0.040		0.044	0.037	0.032	0.044	0.040	0.039	0.005
Fe	0.023		0.023	0.025	0.017	0.024	0.018	0.022	0.004
Mn^{2+}	0.808		0.823	0.825	0.819	0.818	0.815	0.817	0.018
Mn^{3+}	0.227		0.233	0.232	0.238	0.230	0.219	0.231	0.020
Zn	0.072		0.071	0.072	0.075	0.077	0.078	0.074	0.004
Sum	3.000		3.000	3.000	3.000	3.000	3.000	3.000	

Notes: n is the number of point analyses. *Mn^{2+}/Mn^{3+} was calculated to balance four O atoms.

grains analyzed, and in particular the Sb contents remain remarkably constant at 0.50 atoms per formula unit. However, subtle variations exist in the concentration of the remaining major metal ions that in part can be discerned on back-scattered electron images and could allow a discussion of the substitution mechanisms that might be operative. In Figure 3a, Mn^{2+} plus the minor element Zn varies inversely with Mg, i.e., they are to some extent diadochic. A good linear, negative correlation between Ti and Si (correlation coefficient $r = 0.85$) suggests a simple, homovalent Ti^{4+}–Si^{4+} substitution in tegengrenite (Fig. 3b), but simultaneous Fe-Si variations (Fig. 3c) with a fair correlation ($r = 0.67$) indicate more complex, yet unexplained, patterns. The simplified chemical formula for the mineral is given as $(Mg, Mn)_2Sb^{5+}_{0.5}(Mn^{3+}, Si, Ti)_{0.5}O_4$. In reality, the amount of divalent ions is in slight excess of the number indicated by the ideal formula to produce charge balance.

CRYSTALLOGRAPHY

X-ray powder diffraction data

Preliminary studies of tegengrenite with X-ray powder diffraction methods clearly indicated a close relationship to the spinel mineral group. In contrast to the case of filipstadite, where only a few weak superstructure reflections violating the cubic $Fd\bar{3}m$ symmetry were present (Dunn et al. 1988), the diffraction pattern of tegengrenite contains several intense, non-cubic reflections ($I/I_0 = 20\%$) which distinguishes it from those of all previously known spinels sensu lato. From information obtained by electron-diffraction methods, vide infra, the whole pattern could be indexed on a rhombohedral unit cell. The final X-ray powder diffraction data were recorded in the 2θ-range 5–73° on an automated Philips PW1710 diffractometer using graphite-monochromatized Cu$K\alpha$ radiation. Angle positions were corrected against an external Si standard (NBS 640b).

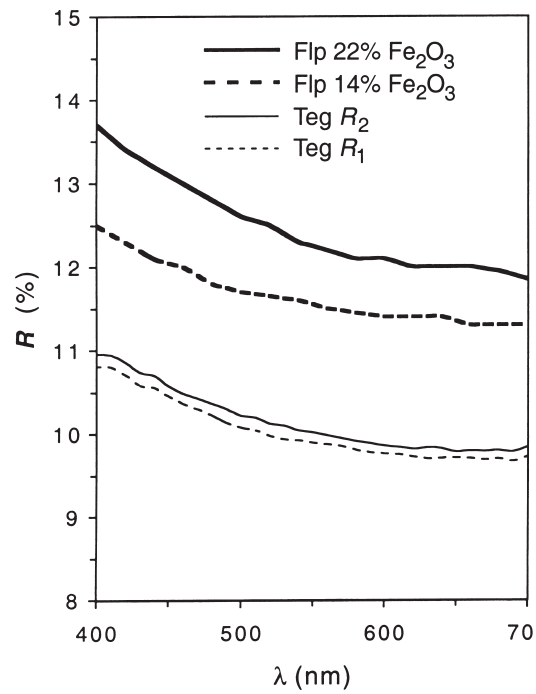

FIGURE 2. Reflectance spectra measured in air for type filipstadite (Flp) and tegengrenite (Teg). The data for filipstadite is from Dunn et al. (1988).

The indexed pattern, including relative peak heights above background, is given in Table 2. The unit-cell parameters (hexagonal setting), refined from forty-four reflections using a least-squares program (Novak and Colville 1989), are $a = 16.196(1)$ Å, $c = 14.948$ (2) Å, and $V = 3395.7(6)$ Å^3. The cubic subcell parameter is $A' = 8.63$ Å.

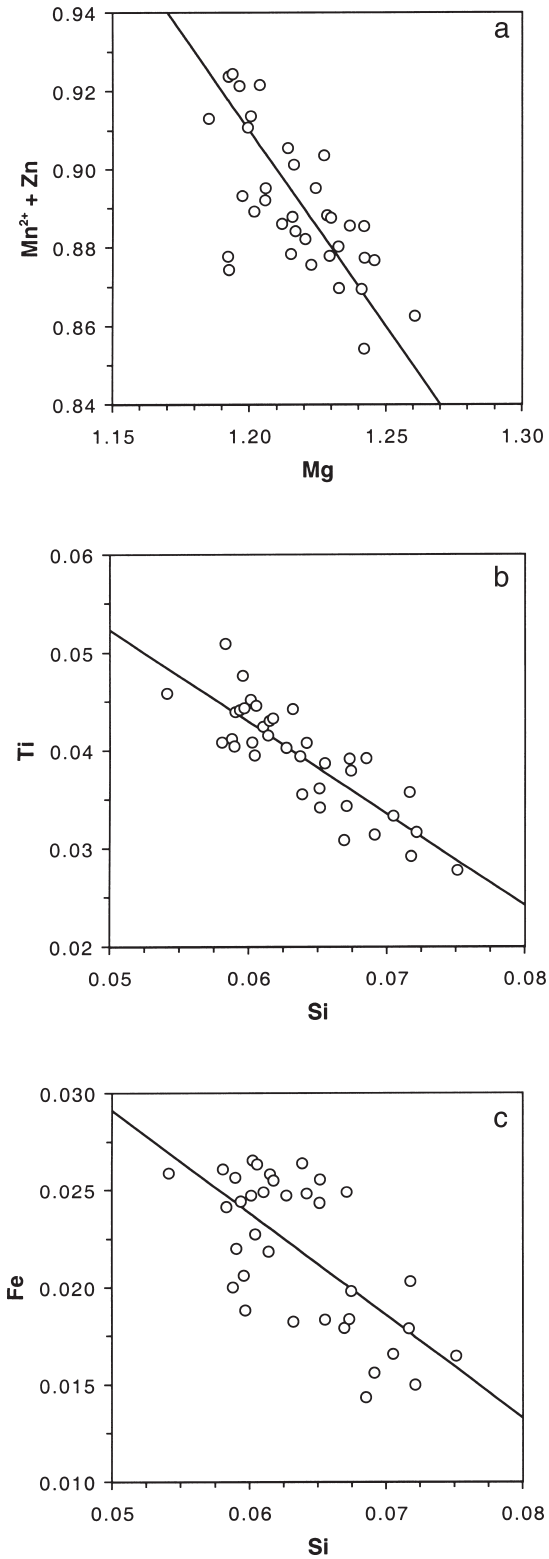

FIGURE 3. Variations of cations in type tegengrenite. (**a**) Divalent species. The solid line serves as guide to the eye, and has a slope of –1.00 and an intercept at 2.11. (**b**) Ti vs. Si. The regression line has a slope of –0.94 and an intercept at 0.099. (**c**) Fe vs. Si. The regression line has a slope of –0.53 and an intercept at 0.055.

X-ray single-crystal diffraction data

With the aim of collecting single-crystal data to be used in future structural refinements, a STOE imaging plate system, mounted on a Siemens rotating Mo anode X-ray generator operated at 50 kV and 90 mA, was used. The recording showed diffraction characteristics of an unusual complexity. All reflections observed can, however, be indexed on a cubic unit cell with **a** = 7**A,** where **A** is the vector defining the cubic subcell. The presence of non-crystallographic extinctions strongly indicated that this was not the true unit cell, but instead domain twinning (supported by the optical observations) was suspected to be the reason for these features of the reciprocal space. A complete conventional refinement of the crystal structure from the data set was thus not possible, and an electron-diffraction study was therefore initiated.

Electron diffraction data

The specimen selected for transmission electron microscopy (TEM) work was prepared by crushing in ethanol, and the fragments obtained were deposited onto a carbon-coated copper grid. Selected area electron diffraction (SAED) patterns were recorded from several different crystallites with a JEOL 2000FX microscope maintained by Stockholm University and operated at 200 kV. Figure 4a shows a SAED pattern along [111] of the spinel subcell. All reflections present can be described as **H** = **G** ± *m***q**, where **G** is the set of Bragg reflections of the spinel-type sublattice, **q** = 1/7 [42$\bar{6}$]* is a (commensurate) modulation wave vector and *m* is an integer, and * denotes a vector in reciprocal space. Note that the three-fold rotation axis is retained but that the mirror plane is not conserved. No higher order Laue zones (HOLZ) caused from any additional superlattice reflections were revealed. The diffraction pattern of tegengrenite can hence be indexed on a rhombohedral unit cell derived from that of spinel, where **a*** = 1/7 (2**A***/3 + 8**B***/3 – 10**C***/3), **b*** = 1/7 (–8**A*** /3 + 10**B***/3 – 2**C***/3), and **c*** = **A***/3 + **B***/3 + **C***/3. Assuming that group-subgroup relations will hold, the space group of tegengrenite can be determined using the path

$$Fd\bar{3}m$$
$$\downarrow\ t4$$
$$\mathbf{a'} = \mathbf{A}/2 - \mathbf{C}/2;\ \mathbf{b'} = -\mathbf{A}/2 + \mathbf{B}/2;\ \mathbf{c'} = \mathbf{A} + \mathbf{B} + \mathbf{C}$$
$$R\bar{3}m$$
$$\downarrow\ t2$$
$$\mathbf{a'}, \mathbf{b'}, \mathbf{c'}$$
$$R\bar{3}$$
$$\downarrow\ i7$$
$$\mathbf{a} = 3\mathbf{a'} + \mathbf{b'},\ \mathbf{b} = -\mathbf{a'} + 2\mathbf{b'},\ \mathbf{c} = \mathbf{c'}$$
$$R\bar{3}$$

Hence, the cell transformation from spinel to tegengrenite is given by **a** = **A** + **B**/2 – 3**C**/2, **b** = –3**A**/2 + **B** + **C**/2 and **c** =

TABLE 2. X-ray powder data for tegengrenite

I/I_0	d_{meas}	d_{calc}	h	k	l
3	10.21	10.23	1	0	1
7	8.07	8.10	1	1	0
3	6.58	6.60	0	1	2
4	6.34	6.35	0	2	1
20	4.98	5.00	2	1	1
		4.98	0	0	3
10	4.67	4.68	3	0	0
19	4.32	4.32	1	2	2
18	4.24	4.24	1	1	3
12	3.761	3.765	1	3	1
2	3.606	3.611	1	0	4
15	3.448	3.451	3	1	2
7	3.408	3.410	3	0	3
8	3.144	3.146	3	2	1
33	3.052	3.061	1	4	0
		3.054	2	1	4
2	2.953	2.956	2	3	2
4	2.756	2.757	0	5	1
7	2.693	2.695	1	3	4
100	2.608	2.610	2	4	1
		2.608	1	4	3
		2.604	1	2	5
8	2.498	2.498	4	2	2
1	2.437	2.438	3	2	4
3	2.387	2.387	1	5	2
3	2.369	2.371	3	1	5
2	2.280	2.279	4	3	1
3	2.246	2.246	5	2	0
28	2.162	2.162	2	4	4
3	2.117	2.117	1	6	1
2	2.089	2.089	5	1	4
2	2.047	2.048	5	2	3
3	1.9857	1.9860	7	0	1
12	1.7679	1.7671	3	6	0
15	1.7663	1.7659	7	0	4
7	1.7617	1.7623	1	2	8
6	1.7414	1.7408	1	7	3
30	1.6652	1.6655	3	6	3
		1.6645	0	7	5
4	1.6195	1.6196	5	5	0
26	1.5313	1.5304	8	2	0
29	1.5273	1.5272	4	2	8
3	1.4891	1.4893	1	7	6
7	1.4633	1.4633	6	5	1
2	1.3685	1.3682	1	9	4
13	1.3202	1.3202	8	4	1
13	1.3167	1.3164	1	2	11
9	1.3049	1.3050	4	8	2
4	1.3026	1.3027	6	6	3

A + B + C. The space-group symmetry of tegengrenite is thus $R\bar{3}$ or, if there is no center of symmetry, $R3$. It also follows that the relation between unit-cell volumes of tegengrenite and the cubic subcell is 21/4. The number of M_3O_4 formula units, Z, in the cell is 8 for spinel and 42 for tegengrenite.

The reflections from the spinel-type sublattice in the SAED pattern of Figure 4a did not change when the crystallite was moved around in the beam (diffraction mode). However, the appearance of the reflections pertaining to the large rhombohedral cell changed radically from one part of the crystallite to another. The difference in appearance between Figures 4a and 4b is attributed to domain twinning.

In the spinel $Fd\bar{3}m$ type cell there are eight equivalent <111> zone axes. In the larger rhombohedral $R\bar{3}$ unit cell six of these directions are minor (low-symmetry) zone axes. In Figure 4a the [001] axis of the rhombohedral structure is proceeding along the [111] spinel axis and in Figure 4b the [001] axis of the rhombohedral structure is proceeding along *another* of the <111> cube axes. The zone axis of this domain would correspond to $[\bar{1}11]$ of the spinel-type sublattice which corresponds to the minor zone axis $[\bar{4},16,7]$ in the rhombohedral unit cell of tegengrenite. Along this axis, the superstructure is not projected and no superstructure reflections are excited in the plane. However, in the outer part of the SAED pattern some reflections of this kind can be observed as HOLZ reflections. It is now clear that the "single crystals" of tegengrenite consist of eight twin domains, a fact which is consistent with the observed X-ray diffraction pattern.

DISCUSSION

As a first approximation, tegengrenite might be considered as the Mg-Mn^{3+} analogue of filipstadite. However, our analyses of several grains consistently show the presence of Si and Ti, albeit in moderate concentrations. We exclude the possibility of submicroscopic silicate phases homogeneously distributed throughout the grains, because they should have been revealed under the TEM. The very constant sums of the tetravalent elements suggest that they are essential components in tegengrenite. In fact, preliminary structural data, based on refinements of one set of superstructure reflections representing a single twin domain of tegengrenite, indicate that Si is indeed ordered at a particular (tetrahedral) site. A fourfold-coordinated site is an unusual environment for Ti^{4+}, but a few cases of $^{[4]}$Si-$^{[4]}$Ti replacement have been documented (e.g., Della Ventura et al. 1996). Although Mg is enriched over Mn in tegengrenite, the proportions of these elements are probably less critical to the stabilization of the phase.

A most interesting aspect of this new mineral is the deviation from cubic symmetry, and that it is the first record of a natural rhombohedral spinel (a few synthetic rombohedral phases inferred to possess spinel-like structures exist, but they are not analogous to tegengrenite). The weakly developed orthorhombic superstructure of type filipstadite was ascribed to the ordering of Sb^{5+} and Fe^{3+} over octahedral sites (Dunn et al. 1988). As Mn^{3+} and Fe^{3+} have practically identical ionic radii (Shannon 1976), the difference in electron configuration is probably involved in the symmetry change from filipstadite to tegengrenite: Mn^{3+} is a d^4 ion and exhibits the co-operative Jahn-Teller effect, which is a common cause to structural distortions in oxides with the spinel structure (e.g., Krupička and Novák 1982). A relevant mineralogical example is the $Fd\bar{3}m \rightarrow I4_1amd$ transition in jacobsite-hausmannite ($MnFe_2O_4$-$MnMn_2^{3+}O_4$).

At the type locality Sb is believed to be syngenetic with Mn and Fe (cf. Holtstam et al. 1998), but due to the high mobility of Sb^{5+}, the element is likely to become redistributed during different stages of metamorphism. The maximum pressure (P) and temperature (T) inferred for the bedrock of the area are about 2 kbar and 650 °C, respectively (corresponding to an amphibolite-facies metamorphic event at 1.85 Ga). On the basis of the textural features (essentially the fact that tegengrenite in many cases has grown on hausmannite as a substrate), tegengrenite crystallized after the metamorphic development of hausmannite, probably in connection with the retrogressive phase that followed. Whatever the exact P and T conditions of formations are, it is obvious that bulk rock composition imposes a strong influence on the nucleation of the mineral. High

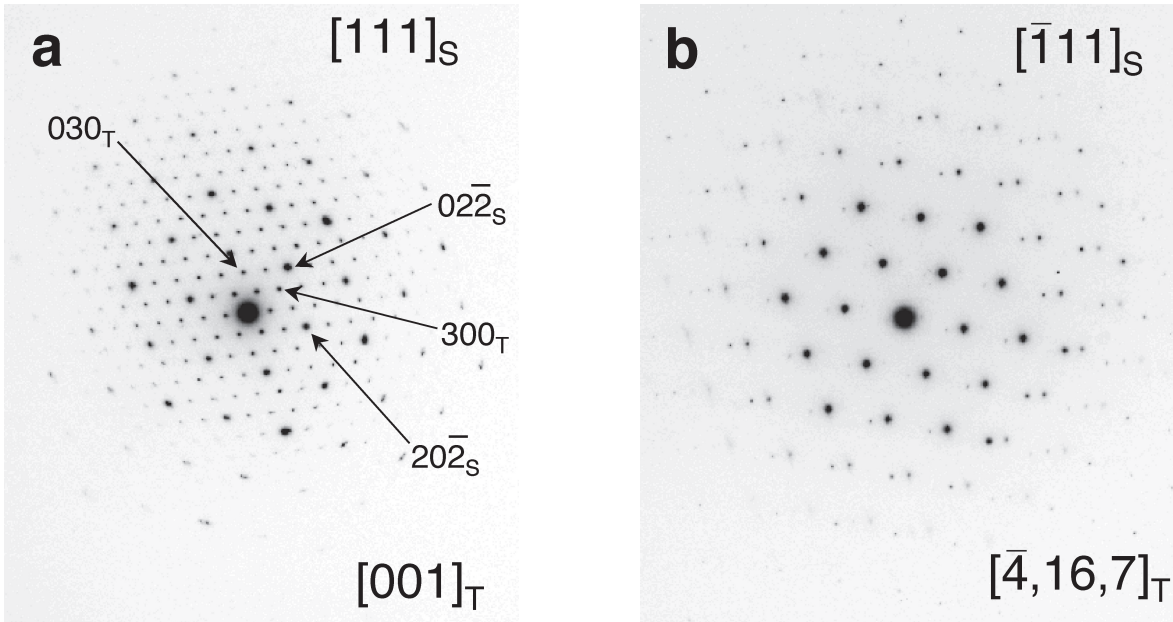

FIGURE 4. SAED patterns from two different domains of a tegengrenite crystal fragment. In (**a**) the pattern is recorded along the [111] zone axis of the spinel (S) subcell which corresponds to the [001] direction of the tegengrenite (T) cell. In the domain of (**b**) the [001] direction of the rhombohedral tegengrenite cell corresponds to another <111> direction in the subcell and the zone axis of the diffraction pattern is instead [$\bar{4}$,16,7].

Mn and Sb concentrations, an increased oxygen fugacity level, and silica undersaturation seem to be instrumental. A low Fe_2O_3 activity is also necessary to suppress filipstadite formation. Tegengrenite must thus be a very rare mineral, although other Långban-type deposits are potential hosts.

ACKNOWLEDGMENTS

T. Lorin is thanked for kindly putting material to our disposal. Financial support was provided by the Swedish Natural Science Research Council (NFR).

REFERENCES CITED

Cervelle, B. and Moëlo, Y. (1990) Reflected-light optics. In D.J. Vaughan and J.L. Jambor, Eds., Advanced microscopic studies of ore minerals, 17, 87–108. Mineralogical Association of Canada Short Course Handbook.

Della Ventura, G., Robert, J.-L., Hawthorne, F.C., and Prost, R. (1996) Short-range disorder of Si and Ti in the tetrahedral double-chain unit of synthetic Ti-bearing potassium-richterite. American Mineralogist, 81, 56–60.

Dunn, P.J., Peacor, D.R., Criddle, A.J., and Stanley, C.J. (1988) Filipstadite, a new Mn-Fe^{3+}-Sb derivative of spinel, from Långban, Sweden. American Mineralogist, 73, 413–19.

Holtstam, D. (1993) A second occurrence of filipstadite in Värmland, Sweden. Geologiska Föreningens i Stockholm Förhandlingar, 115, 239–240.

Holtstam, D. and Langhof, J., Eds. (1999) Långban. The mines, their minerals, geology and explorers, 218 p. Raster Förlag, Stockholm.

Holtstam, D. and Norrestam, R. (1993) Lindqvistite, $Pb_2Me^{2+}Fe_{16}O_{27}$, a novel hexagonal ferrite mineral from Jakobsberg, Filipstad, Sweden. American Mineralogist, 78, 1304–1312.

Holtstam, D., Nysten, P., and Gatedal, K. (1998) Parageneses and compositional variations of Sb oxyminerals from Långban-type deposits in Värmland, Sweden. Mineralogical Magazine, 62, 395–407.

Krupička, S. and Novák, P. (1982) Oxide spinels. In E.P. Wohlfahrt, Ed., Ferromagnetic Materials, vol. 3, p. 305–391. North-Holland Publishing Company, Amsterdam.

Mandarino, J.A. (1981) The Gladstone-Dale relationship. IV. The compatibility concept and its application. Canadian Mineralogist, 19, 441–450.

Moore, P.B. (1970) Mineralogy & chemistry of Långban-type deposits in Bergslagen, Sweden. Mineralogical Record, 1, 154–172.

Novak, G.A. and Colville, A.A. (1989) A practical interactive least-squares cell-parameter program using an electronic spreadsheet and a personal computer. American Mineralogist, 74, 488–490.

Pouchou, J.L. and Pichoir, F. (1984) A new model for quantitative X-ray microanalysis. I. Application to the analysis of homogeneous samples. La Recherche Aérospatiale, 3, 13–36.

Shannon, R.D. (1976) Revised effective ionic radii and systematic studies of interatomic distances in halides and chalcogenides. Acta Crystallographica, A32, 751–767.

Tegengren, F. (1921) The iron ores and iron industry of China. Geological Survey of China, A2(1), 1–457.

———(1924) Sveriges ädlare malmer och bergverk. Sveriges geologiska undersökning, Ca17, 1–406.

MANUSCRIPT RECEIVED DECEMBER 14, 1999
MANUSCRIPT ACCEPTED APRIL 20, 2000
PAPER HANDLED BY GERALD GIESTER